

# MICROSCOPE INSTRUMENT DEVELOPMENT, LESSONS FOR GOCE

PIERRE TOUBOUL

*Physical Instrumentation Department, ONERA, F-92322 Chatillon Cedex, France*  
(touboul@onera.fr)

Received: 4 November 2002; Accepted in final form: 27 November 2002

**Abstract.** Two space missions are presently under development with payload based on ultra-sensitive electrostatic accelerometers. The GOCE mission takes advantage of a three axis gradiometer accommodated in a very stable thermal case on board a drag-free satellite orbiting at a very low altitude of 250 km. This ESA mission will perform the very highly accurate mapping of the Earth gravity field with a geographical resolution of 100 km. The MICROSCOPE mission is devoted to the test of the “Universality of free fall” in view of the verification of the Einstein Equivalence Principle (EP) and of the search of a new interaction. The MICROSCOPE instrument is composed of two pairs of differential electrostatic accelerometers and the accelerometer proof-masses are the bodies of the EP test. The satellite is also a drag-free satellite exhibiting a fine attitude control and in a certain way, each differential accelerometer is a one axis gradiometer with an arm of quite null length. The development of this instrument much interests the definition and the evaluation of the sensor cores of the gradiometer. The in flight calibration process of both instruments is also very similar. Lessons from these parallel developments are presented.

## 1. Introduction

In the last decade, several space missions have involved very high sensitive accelerometers with a resolution better than 1 nano- $g$  (1  $g$  = Earth mean gravity field on ground). In the SpaceLab flying on board the COLUMBIA shuttle, the survey at low frequency (down to 0.1 mHz) of the residual acceleration level has been performed twice for dedicated micro-gravity experiment missions with electrostatic three-axes accelerometers (Nati *et al.*, 1994; McPherson *et al.*, 1999) down to a level of one nano- $g$ .

The CHAMP and the GRACE satellites have been launched respectively in July 2000 and March 2002 and carry at their centre of mass such an instrument for the fine measurement of the surface forces acting on the satellites (Reigber *et al.*, 1996; Reigber *et al.*, 2002; JPL, GRACE, 1998; Tapley and Reigber, 2002). CHAMP is the precursor of this new generation of space geodesy missions, all considering on board measurements of the acceleration or gravity field. The two GRACE satellites are flying on the same orbit, injected at 480 km with a 98° inclination and a separation distance of about 230 km. The relative velocity of the satellite is as low as 1 km per day. The fine spacecraft trajectography is performed by the on board GPS receivers and the relative motion of the satellite is measured by one accurate micro-wave tracking, leading, with the accelerometer outputs together



to the recovery of the monthly variations of the Earth gravity field. The required performance for the accelerometer is  $10^{-10} \text{ ms}^{-2}$  over 1 second integration period.

Two new space missions are now under development respectively in ESA and CNES, requiring sensors with improved performance by a factor one hundred. The GOCE mission takes advantage of a three axis gradiometer accommodated on board a drag-free satellite orbiting at a very low altitude of 250 km; the atmospheric drag of the satellite is so compensated by the continuous and controlled thrust of the electrical propulsion system (ESA, 1999). This ESA mission will perform the very accurate mapping of the Earth gravity field with a geographical resolution of 100 km. Each of the three one axis gradiometer constituting the instrument, is composed of a very steady structure and two highly sensitive inertial sensors mounted at the two ends, half a meter distance from each other.

The MICROSCOPE mission, also scheduled for a launch in 2006, is devoted to the test of the “Universality of free fall” in view of the verification of the Einstein Equivalence Principle (EP) or of the search of a new interaction (Touboul *et al.*, 2002). The MICROSCOPE instrument is composed of two pairs of differential electrostatic accelerometers and the accelerometer proof-masses are the bodies of the EP test. The satellite is also a drag-free satellite exhibiting a fine attitude control and in a certain way, each differential accelerometer is a one axis gradiometer with an arm of quite null length. The expression of the performed measurements are very similar in both cases but in MICROSCOPE the gravity gradient is the disturbing signal while in GOCE, it is the signal to be measured. The developments of both instruments are also comparable because of the same concept of operation and of the same approach to increase the resolution from the already existing accelerometers presently in orbit. This is in particular possible because of the limited range of operation thanks to the vibration soft environment provided by the drag-free satellite and of the very stable thermal environment inside the controlled instrument case. Some lessons from the MICROSCOPE instrument development are thus pointed out to assess the selected configuration for the GOCE gradiometer.

## 2. MICROSCOPE Mission

More accurate experiments confirming the equivalence between inertial mass and gravitational mass represent important verifications of the relativity theory of gravitation and other metric theories, which postulate this principle. The search of a new interaction (with extra mass-less scalar field in particular) expected by the string theories in view of a quantum gravity theory is also a great and recent motivation for ground and space experiments in addition to the determination with better accuracy of the Post Newtonian coefficients (Damour *et al.*, 2002; Lämmerzahl *et al.*, 2000).

The MICROSCOPE mission (MICROSatellite pour l’Observation du Principe d’Equivalence), has been selected by CNES with three other micro-satellite mis-

sions devoted to Earth observation DEMETER, PARASOL and PICARD (CNES, 2002). This fundamental physics space experiment aims at the EP test with an expected accuracy of at least  $10^{-15}$ , more than two orders of magnitude better than the last ground tests performed with torsion pendulum and limited by the Earth gravity gradient, the seismic noise and the disturbances induced by human activities (Fischbach and Talmadge, 1998).

Recent altimetry and geodesy missions lead to the global and accurate determination of the Earth gravity field expressed with spherical harmonics series and to the production of dedicated mathematical and computational tools for the simulation of accurate orbital motion. Micro-satellites with a mass limited to 150 kg maximum are now available with low cost launch opportunities like ARIANE V secondary small passengers or Russian or Ukrainian launchers. In addition, the experience of the measurement of weak accelerations by electrostatic accelerometers performed on board the CHAMP and the GRACE satellites confirm the way of a fast and cheap space experiment devoted to the EP test and preparing more ambitious other missions in fundamental physics (Touboul *et al.*, 1998; Touboul, 2000).

The MICROSCOPE experiment consists in maintaining two test masses made of different materials along the same orbit. The relative motion of the two masses is finely measured and electrostatic fields are generated all around each mass to apply well controlled electrostatic pressures. The symmetry of the configuration is of peculiar importance. The two masses are cylindrical and concentric (their centre of mass at the same point) in such a way that they are submitted to the same Earth gravity field. In case of no violation of the EP, the electrostatic fields, controlled around the mass generate the same acceleration. These electrostatic accelerations are finely measured along the Earth pointing axis that is projected along the three instrument axes according to the satellite attitude. So, when the satellite is inertial pointing or orbiting about the normal axis to the orbital plane, the EP signal to be detected will be modulated respectively at the orbital frequency or at the sum (or difference according to the sign of the satellite rotation) of the spin and orbital frequency, *i. e.* between  $1.7 \times 10^{-4}$  Hz and a few  $10^{-3}$  Hz.

### 3. MICROSCOPE Instrument and Accommodation

The satellite payload is composed in fact of two quite identical differential electrostatic accelerometers, each of the two pairs of masses being the two proof-masses of two accelerometers. The masses are made of the same Platinum Rhodium alloy for the first one, dedicated to assess the accuracy of the experiment: for a perfect experiment, the outputs of the two accelerometers are identical. The materials are Platinum Rhodium alloy and Titanium or Copper alloy for the second one. Then, in view of suppressing the systematic errors, the experiment logic relies on the double

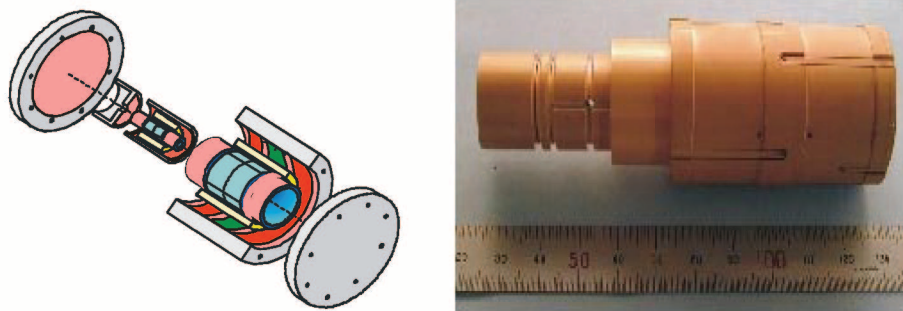


Figure 1. Differential accelerometer configuration: each of the two masses, in yellow, are integrated inside a silica core composed of the inner and the outer cylinders which carry the electrodes: radial in blue on the internal cylinder and axial in red on the external one (left picture). Prototype of the inner inertial sensor (right picture).

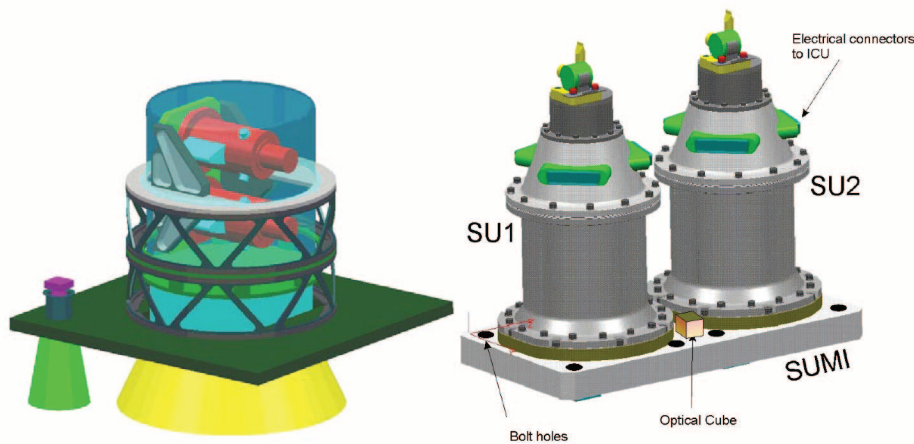


Figure 2. Accommodation of the two tight housings (right) inside the double-stage thermal insulated case of the payload (left). The yellow cone is turned normal to the orbital plane, to the opposite of the Sun. It protects the external radiator of the payload case from the Earth radiation fluctuations in order to increase its temperature stability and so the temperature of the payload especially at the  $f_{EP}$  frequency.

comparison of the outputs of two pairs of electrostatic accelerometers. The weight of the masses ranges from 0.4 kg up to 1.7 kg.

One differential accelerometer is composed of two concentric electrostatic inertial sensors (see Figure 1) with fused silica cylindrical cage carrying sets of electrodes engraved in the cage gold coatings all around the mass. The configuration of the electrode set presents an axial and a radial symmetry.

Pairs of electrodes are used for the capacitive sensing of the mass position and attitude along the three axes (Josselin *et al.*, 1999). The same electrodes are used to generate the electrostatic fields around the mass for the control of its motion. The eight quadrant electrodes concern the radial translations and rotations. The

two cylindrical sensing electrodes located at the ends of the test-mass are used for the axial direction. The rotation of the mass about the axial direction is measured through dedicated flat areas on the mass and external electrodes in regard.

The cylindrical configuration allows the centering of the two masses at the same point to suppress the effect of the satellite or the Earth gravity gradients. It is also optimised for the reduction of the electrostatic stiffness and damping associated to the mass motion along the axial direction to the benefit of performance of the one major axis along which the EP test is performed. The mean electrostatic force applied on both masses is in fact nullified by the satellite drag compensation system that acts through a servo-loop on the thrusters of the satellite which so follows the masses.

The position and the attitude of the masses can be finely adjusted by offsetting the six servo-loops which performs from the capacitive sensing the electrostatic control of the mass with respect to the instrument frame. The instrument sensitivity to the mass relative position will be verified during the calibration phase as well as the rejection rate of the Earth gravity gradient signal depending on it.

As shown in Figure 2 (right), the instrument cores are integrated in tight vacuum housings that provide also thermal insulation and magnetic shielding. The two housings, mounted on a rigid structure, are then accommodated inside a double stage thermal case. The satellite external structure, in green on the left picture, carries the star sensors that have to be steadily aligned with the inertial sensor (better than 1 arc min): the control of the satellite attitude is performed from the complementary pointing measures provided by the star sensors and the angular acceleration measures provided by the inertial sensors. The passive thermal control of the sensor units and the associated electronics must meet the requirements expressed in Table I.

These requirements are deduced from the accelerometer thermal sensitivity considering the thermal expansion of the mechanical parts, the sensitivities of the electronics components, the radiation pressures and the radiometric force applied on the masses, plus other minor effects. Obviously, these effects have to be considered about the EP signal frequency,  $f_{EP}$ , for the MICROSCOPE mission, and then expressed in power spectral density or at the EP signal frequency (tone). Not only the sine but also the phase of the eventual violation signal is well known because it has to correspond to the Earth gravity monopole direction. Thus, random perturbations can be filtered out through heterodyne detection. This will not be the case of the GOCE mission for which the gravity signal variations to be measured extends in a frequency bandwidth up to 0.1 Hz.

The differential accelerometer housings are mounted near the satellite centre of mass but contrarily to missions like CHAMP or GRACE, no stringent requirement with millimeter accuracy is demanded. In these previous missions, the accelerometer outputs are representative to the external surface forces acting on the satellite and exploited to analyse the orbital motion of the satellite centre of mass: centering the instrument is required to reject the impact of the centrifugal and the angular

TABLE I

Comparison of the thermal environment requirements for the instrument sensor core and the electronics units in case of the MICROSCOPE and the GOCE missions. Power Spectral Density (PSD) and tone variations are defined at the interface of the mounting plane. Each unit benefits in addition from its own thermal insulation and inertia.

	MICROSCOPE Electronics unit	MICROSCOPE Mechanics unit	GOCE Electronics unit	GOCE Mechanics unit
Operating temperature	+10°C to +50°C	+20°C to +40°C	+20°C to +30°C	+20°C to +25°C
Thermal variations:				
PSD	2 K Hz <sup>-1/2</sup> (about $f_{EP} \sim 10^{-3}$ Hz)	200 mK Hz <sup>-1/2</sup> (about $f_{EP} \sim 10^{-3}$ Hz)	10 mK Hz <sup>-1/2</sup> ( $5 \times 10^{-3}$ Hz-0.1 Hz)	5 mK Hz <sup>-1/2</sup> ( $5 \times 10^{-3}$ Hz-0.1 Hz)
Tone (sine at $f_{EP}$ )	6 mK	0.6 mK	Not applicable	Not applicable
Thermal Gradients:				
PSD	Not applicable	2 K/m Hz <sup>-1/2</sup> (about $f_{EP} \sim 10^{-3}$ Hz)	Not applicable	125 mK/m Hz <sup>-1/2</sup>
Tone (sine at $f_{EP}$ )	Not applicable	6 mK/m	Not applicable	Not applicable

accelerations of the satellite and of the gravity gradient. In the case of the MICROSCOPE mission, as well as of the GOCE one, the drag free point of the satellite (*i.e.* falling around the Earth) is defined by the satellite torque and force compensation system. And this point is defined from the accelerometer outputs themselves, so independently of the satellite centre of mass but of the accelerometer proof-masses.

#### 4. MICROSCOPE Differential Measurement

The measure provided by one differential accelerometer can be expressed from the equation of the two mass motions:

$$m_{I_A} (\ddot{X}_A + \ddot{x}_A) - m_{g_A} g_A = F_A + F_{p_A}$$

with  $I$ ,  $g$  and  $A$  (or  $B$  later), the inertial or the gravitational mass  $A$  (or  $B$ ),  $X$  the motion of the instrument frame (or of the satellite) with respect to the inertial frame,  $x$  the motion of the proof-mass with respect to the instrument frame,

$$g_i = -\frac{\mu (X_i + x_i)}{r^2}$$

gravity field (2) and

$$T_{ij} = -\frac{\mu}{r^3} \left( \delta_{ij} - \frac{3(X_i + x_i)(X_j + x_j)}{r} \right)$$

gravity gradient tensor (3) with  $\mu \approx 4 \times 10^{14} \text{ m}^3\text{s}^{-2}$ , the Earth gravitational constant and  $r$  the distance to the geocentre,  $r = \left( \sum_{i=1}^3 (X_i + x_i)^2 \right)^{1/2}$  ( $X_i + x_i$ ) the rectangular co-ordinates of the current point in Earth's fixed orthonormal frame;  $\delta_{ij}$  is the Kronecker symbol;  $g_A$  the Earth gravitational field integrated over the mass volume  $A$ ,  $F_A$  and  $F_{p_A}$ , are the forces respectively applied by the electrostatic suspension or by the disturbing sources.

The electrical signal delivered by each inertial sensor is representative of the electrostatic force  $F_A$ :

$$\hat{F}_A = (I + K_A)F_A + E(F_A) + E_{n_A}$$

with  $I$  and  $K_A$ , respectively the identity and the sensitivity matrix,  $E(F_A)$  and  $E_{n_A}$ , respectively the nonlinearity and the noise of the measurement system.

Then, by performing the difference of the inertial sensor outputs:

$$\begin{aligned}
\frac{\hat{F}_A}{m_{I_A}} - \frac{\hat{F}_B}{m_{I_B}} \approx & +(K_A - K_B) \frac{\ddot{X}_A + \ddot{x}_A + \ddot{X}_B + \ddot{x}_B}{2} + \left( I + \frac{K_A + K_B}{2} \right) \\
& \times (\ddot{X}_A - \ddot{X}_B) + \left( I + \frac{K_A + K_B}{2} \right) \\
& \times \{ (\ddot{x}_A^\circ - \ddot{x}_B^\circ) + 2\Omega (\dot{x}_A - \dot{x}_B) + (\Omega\Omega + \dot{\Omega})(x_A - x_B) \} \\
& - \frac{\hat{F}_{\rho A}}{m_{I_A}} + \frac{\hat{F}_{\rho B}}{m_{I_B}} + \frac{E(F_A)}{m_{I_A}} - \frac{E(F_B)}{m_{I_B}} + \frac{E_{nA}}{m_{I_A}} - \frac{E_{nB}}{m_{I_B}} \\
& - \frac{1}{2} \left( \frac{m_{gA}}{m_{I_A}} + \frac{m_{gB}}{m_{I_B}} \right) (g_A - g_B) \\
& - \left( \frac{m_{gA}}{m_{I_A}} - \frac{m_{gB}}{m_{I_B}} \right) \left( \frac{g_A + g_B}{2} \right) \tag{1}
\end{aligned}$$

The first term of the first line corresponds to the common mode acceleration not fully suppressed in the difference because of the non equal sensitivity matrices. The second and third terms corresponds respectively to the relative residual motion of the masses (limited by the stability of the instrument assembly) and to the effect of the instrument attitude variations,  $\Omega$  being the angular velocity about the drag free point (time derivatives noted  $^\circ$  are performed in the rotating frame).

The fourth line depends only on the inertial sensor noises and defects. Motions of the test-masses are measured along the axis of revolution (peculiar sensitive axis) with a resolution of  $6 \times 10^{-10}$  m/ $\sqrt{\text{Hz}}$  and controlled with a resolution around  $1.5 \times 10^{-12}$  m/s<sup>2</sup>/ $\sqrt{\text{Hz}}$  for an operating range reduced to  $5 \times 10^{-7}$  m/s<sup>2</sup>. The first source of limitation of the resolution at the frequency  $f_{EP}$  is the fluctuation-dissipation noise induced by the proof-mass motion damping due to the thin gold wire used for the charge control of the mass:

$$\Gamma_{\text{wire}}^2 = \left( \frac{1}{m} \sqrt{4k_b T \frac{k_{\text{wire}}}{2\pi f_{EP} Q_{\text{wire}}}} \right)^2 (\text{ms}^{-2})^2/\text{Hz}$$

with  $Q_{\text{wire}}$  measured greater than 100 and  $k_{\text{wire}}$  lower than  $5 \times 10^{-6}$  N/m (Willemont and Touboul, 1999). The same charge control is performed for the GOCE accelerometer mass, where the same limitation at lower frequency is encountered. The fourth term corresponds to the gravity gradient signal and the last one to the eventual EP signal.

The atmospheric and thermal drag and torque of the satellite as well as others are actively compensated by the continuous controlled variations of the thrust of the electrical propulsion such that the satellite follows the two test masses in their gravitational motion with residual motion fluctuations of  $3 \times 10^{-10}$  m/s<sup>2</sup>/ $\sqrt{\text{Hz}}$  in translation and  $10^{-8}$  rad/s<sup>2</sup>/ $\sqrt{\text{Hz}}$  in rotation. The propulsion system allows also a fine calibration of the instrument by generating well known kinematic accelerations



in all six degrees of freedom. This allows to verify the sensitive axis alignments and the matching of the instrument sensitivities necessary to reject the common kinematic acceleration fields ( $K_{A_{ij}} - K_{B_{ij}} < 3 \times 10^{-4}$ ). The same approach is considered in the GOCE mission except that the drag-free point is at the gradiometer centre and not at the test mass unique centre.

The selection of a 6–18 hour helio-synchronous orbit leads to the avoidance of fluctuations of the Sun orientation and the eclipse during the mission measurement phase, reducing the temperature variations and the thermo-elastic structural constraints which can generate spikes of acceleration. The same orbit is selected for GOCE but at lower altitude to the benefit of the gradiometer resolution but so with unfortunately many eclipses. The eccentricity of the quasi circular orbit must be sufficiently small to concentrate the power spectrum of the Earth monopole gravity field in one major spectral line. Furthermore, the fluctuations of the gravity gradient in the instrument frame has to be confined to the same spectral line.

The perturbing effect of the satellite and the Earth gravity gradient is of peculiar importance. The cylindrical test masses present sphere-like inertia matrices to limit these effects and the off-centering of the two masses is limited by construction to  $20 \mu\text{m}$ ; gravity attractions are then equal on both masses with an accuracy of better than one part per thousand, which is sufficient for the experiment according to the environment. Moreover, the in orbital plane off-centering can be evaluated in flight with an accuracy better than  $0.1 \mu\text{m}$  through the measured effect of the gravity gradient major component at twice the frequency of the gravity field.

Thus the orbit eccentricity must be smaller than  $5 \times 10^{-3}$  to limit at  $f_{EP}$  the disturbing difference of accelerations induced by the gravity gradients (in case of inertial pointing satellite; for a rotating satellite, the disturbing effect is modulated and so no more at  $f_{EP}$ ). In this process, the knowledge of the satellite position is necessary to compute the gravity gradient:  $300 \text{ m}$  can be achieved along the three directions and appears sufficient. The out of plane off-centering cannot be estimated in orbit through the gravity gradient data analysis, thus the  $20 \mu\text{m}$  initial value has to be considered when specifying the instrument axis direction in the orbital plane. Instrument frame, orbital plane and satellite rotation axis shall thus be aligned with a few  $10^{-3}$  rd accuracy.

All these mission requirements correspond to the objective of  $10^{-15}$  EP test accuracy, *i.e.* the detection at  $f_{EP}$  and in phase of any signal as weak as  $8 \times 10^{-15} \text{ ms}^{-2}$ , an integration period of  $10^5 \text{ s}$  being considered.

## 5. GOCE Gradiometry Mission

The GOCE (Gravity field and steady-state Ocean Circulation Explorer) mission was selected in 1999 as the first core mission of the Earth Explorer programme of ESA (European Space Agency). After numerous studies for more than two decades (Bernard *et al.*, 1983; Rummel and Colombo, 1985; Touboul *et al.*, 1991; Balmino

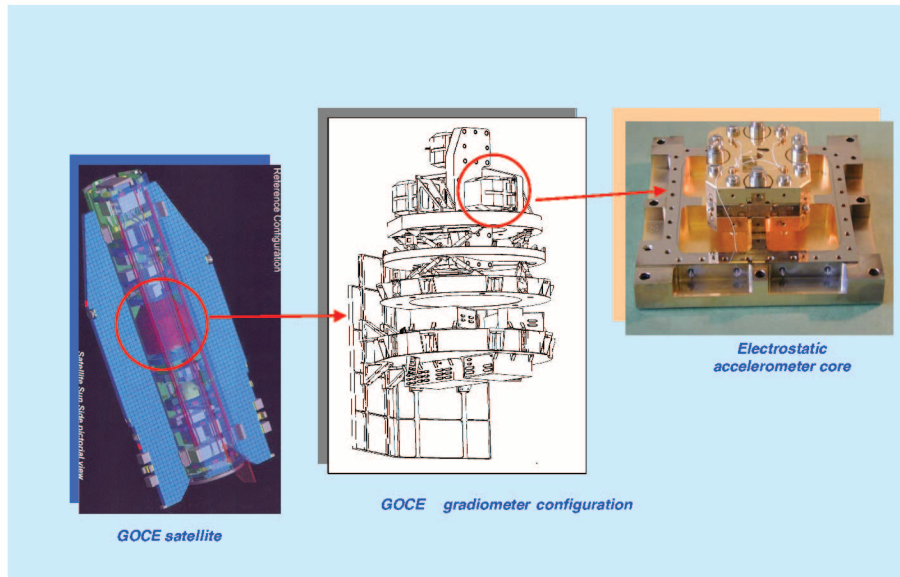


Figure 3. GOCE payload configuration. The satellite carries at its centre the gradiometer case with two thermally controlled housings. The gradiometer is composed of a rigid diamond structure, 6 inertial sensor cores and 4 electronics units, one per gradiometer axis plus a main interface unit.

and Perosanz, 1997), GOCE will fly for the first time a gradiometer on board a drag-free satellite at a very low altitude around 250 km (see Figure 3). The orbit inclination is  $96.5^\circ$  corresponding to an heliosynchronous orbit, 6h–18h for full and steady solar pointing. In fact, the satellite will be injected at a safer altitude of 270 km where the operations of all sub-systems and in particular the drag compensation will be verified before decreasing the altitude to 250 km and 240 km for two phases of measurements. The satellite cross section is minimum to reduce the drag to be compensated and the solar panels are rigidly mounted on the satellite like for the MICROSCOPE satellite.

The gradiometer instrument, designed by ONERA in the last decade, includes six up-to-date ultra-sensitive electrostatic accelerometers capable of measuring accelerations as weak as  $4 \times 10^{-13} \text{ ms}^{-2}$  with 10 s integrating time. The gradiometer will deliver the three diagonal components of the gravity gradient tensor,  $T$ , in the Earth pointing spacecraft axes, with an accuracy of a few milli-Eötvös/Hz<sup>1/2</sup> (1 Eötvös =  $10^{-9} \text{ s}^{-2}$ ), the frequency measurement bandwidth being from 0.005 Hz up to 0.1 Hz. The satellite is also tracked by the GPS satellite net and by ground laser stations, actually like CHAMP and GRACE. The fine trajectory recovery associated to the gradiometer measures is expected to conduct to a global gravity model with a resolution of at least 100 km and a total uncertainty of 2.5 millimeters on the geoid and 0.1 milligal on the gravity. This will therefore be an outstanding accurate reference for the concerned disciplines: geodesy, solid Earth physics,

oceanography and climatology. GOCE is scheduled for a launch at beginning of 2006.

The GRADIO accelerometer devoted to space gradiometry is in fact directly derived from the STAR and SuperSTAR accelerometers of respectively the CHAMP and the GRACE missions with quite the same mechanical core configuration and electrical architecture, which is well suited to realise a three-axes accelerometer with the possibility to perform ground tests under normal gravity. The parallelepiped proof-mass of 4 cm side and 1 cm height is made in Platinum-Rhodium instead of Titanium increasing the mass from 72 grams to 320 grams to the benefit of the rejection of the parasitic forces applied directly on the mass independently of the electrostatic suspension. The same technology as for the previous missions and for MICROSCOPE are implemented with gold coated ULE parts. The asymmetry of the configuration (not a cubic proof-mass) is required to perform the electrostatic suspension of the mass under one  $g$ , the electrode areas being larger along the vertical and the distance between the proof-mass and the electrodes 10 times less than in the two other directions, *i.e.* 30  $\mu\text{m}$ . An electrostatic field as strong as  $3 \times 10^7$  V/m is necessary to sustain the proof-mass. This axis will have in flight less performance than the two others (about a factor 300) with a greater full range and a stiffer mass control.

The electronics is made on the basis of the already developed circuits for the capacitive sensing and for the generation of the suspension control voltages. Optimal settings are defined according to the needed maximum range of operation that is forced by the DC gravity gradient to be sustained while the drag-free point is at the centre of the gradiometer. Contrarily to MICROSCOPE, this range is necessarily greater than a few  $10^{-6} \text{ ms}^{-2}$  and the stability of the accelerometer scale factor at level of  $10^{-7}$  is mandatory for the two ultra-sensitive axes.

The thermal stability of the gradiometer case is thus demanded not only to preserve the stability of the sensor sensitivity and bias but also the geometry of the structure and the mounting parts. Table I compares the requirements with respect to the MICROSCOPE ones. While the GOCE requirements are more stringent in term of random fluctuations because of the huge signal to noise ratio to be reached, more than  $10^6$  even for the difference of the two measures of acceleration (from the DC gravity gradient of a few thousand Eötvös to the objective in milli-Eötvös per  $\text{Hz}^{-1/2}$ ), the MICROSCOPE experiment demands also a peculiar care on the temperature fluctuations at the experiment frequency and in phase with the eventual EP violation signal.

## 6. GOCE and MICROSCOPE Similar Driving Parameters

The expression of the measure provided by each one axis gradiometer is identical to equation (1) but the Eötvös ratio (gravitational over inertial mass) is assumed

one:

$$\begin{aligned}
\frac{\hat{F}_A}{m} - \frac{\hat{F}_B}{m} \approx & +(K_A - K_B) \frac{\ddot{X}_A + \ddot{x}_A + \ddot{X}_B + \ddot{x}_B}{2} + \left( I + \frac{K_A + K_B}{2} \right) \\
& \times (\ddot{X}_A - \ddot{X}_B) + \left( I + \frac{K_A + K_B}{2} \right) \\
& \times \left\{ (\ddot{x}_A - \ddot{x}_B) + 2\Omega(\dot{x}_A - \dot{x}_B) + (\Omega\Omega + \dot{\Omega})(x_A - x_B) \right\} \\
& - \frac{\hat{F}_{pA}}{m} + \frac{\hat{F}_{pB}}{m} + \frac{E(F_A)}{m} - \frac{E(F_B)}{m} + \frac{E_{nA}}{m} - \frac{E_{nB}}{m} \\
& - (g_A - g_B)
\end{aligned} \tag{2}$$

The expected resolution of the accelerometer is  $10^{-12} \text{ ms}^{-2}/\text{Hz}^{-1/2}$ , along the gradiometer axis and the second ultra-sensitive axes, in the gradiometer measurement bandwidth of ( $5 \times 10^{-3} \text{ Hz} - 0.1 \text{ Hz}$ ) corresponding to about 1400 km–70 km track distance. As for the MICROSCOPE inertial sensor configuration, the resolution is limited at low frequency by the damping induced by the gold wire used for the mass charge control. In the upper frequency band, the limitation of the resolution is the noise,  $x_{\text{noise}}$ , of the proof-mass capacitive sensing: this acceleration noise source increases to the power 4 of the signal frequency  $f_{\text{sig}}$  (in PSD).

$$\Gamma_{\text{posnoise}}^2 = x_{\text{noise}}^2 \left( 4\pi^2 f_{\text{sig}}^2 + 4\pi^2 f_p^2 \right)^2 (\text{ms}^{-2})^2/\text{Hz}$$

with  $f_p$  the frequency of the residual stiffness between the mass and the instrument frame, managed lower than  $f_{\text{sig}}$  by the selection of the electrostatic configuration and the diameter of the gold wire ( $5 \mu\text{m}$ ).

In fact, in spite of the difference of the geometrical configuration, the intrinsic performance of the inertial sensors are very similar along the ultra-sensitive axes.

In GOCE, as in MICROSCOPE, all accelerometer outputs are also used for the drag compensation and the attitude control of the satellite. Because of the limited matching of the sensitivity matrices, both missions are very demanding for this satellite system. Table II summarises the established requirements in line with the mission objectives. Obviously, the frequency aspects are different for the two missions and MICROSCOPE is only demanding for the rejection of the disturbing line at the EP test frequency.

The requirement for the satellite pointing and positioning comes from the difference of the expression of the Earth gravity gradient tensor in the actual or the evaluated frame of measurement. Because in MICROSCOPE, this disturbing signal is limited by the mass centering ( $20 \mu\text{m}$  instead of 0.5 m), the requirements are less stringent. The sensitivity matrices of the MICROSCOPE sensors are expected to be matched in orbit with a  $3 \times 10^{-4}$  relative accuracy and a  $10^{-5}$  accuracy for the GOCE mission. The calibration process has been demonstrated in laboratory as shown in Figure 4. This more accurate calibration is necessary but also possible

TABLE II  
Satellite controls. Both satellites are drag free thanks to Field Effect Electrical Propulsion and Ion thrusters. GOCE lower altitude (250 km, three times lower) requires much more control strength.

	MICROSCOPE	GOCE	GOCE
		Normal to the orbit plane	Along the orbital plane axes
Satellite position	300 m	0.5 m	0.5 m
Satellite pointing	$10^{-3}$ rd; $3 \times 10^{-3}$ rdHz $^{-1/2}$	$7 \times 10^{-4}$ rd; $2 \times 10^{-5}$ rdHz $^{-1/2}$	$7 \times 10^{-4}$ rd; $2 \times 10^{-5}$ rdHz $^{-1/2}$
Satellite residual drag	$3 \times 10^{-10}$ ms $^{-2}$ Hz $^{-1/2}$	$2.5 \times 10^{-8}$ ms $^{-2}$ Hz $^{-1/2}$	$2.5 \times 10^{-8}$ ms $^{-2}$ Hz $^{-1/2}$
Angular velocity:	Inertial pointing or Rotating at $10^{-3}$ rds $^{-1}$		
PSD	$10^{-6}$ rds $^{-1}$ Hz $^{-1/2}$ (about $f_{EP} \sim 10^{-3}$ Hz)	Earth pointing: $1.2 \times 10^{-3}$ rds $^{-1}$ $10^{-6}$ rds $^{-1}$ Hz $^{-1/2}$ ( $5 \times 10^{-3}$ Hz-0.1Hz)	$10^{-5}$ rds $^{-1}$ $5 \cdot 10^{-7}$ rds $^{-1}$ Hz $^{-1/2}$ ( $5 \times 10^{-3}$ Hz-0.1Hz)
Tone (sine at $f_{EP}$ )	$2 \times 10^{-8}$ rds $^{-1}$	Not applicable	Not applicable
Angular acceleration:			
PSD	$10^{-8}$ rds $^{-2}$ Hz $^{-1/2}$ (about $f_{EP} \sim 10^{-3}$ Hz)	$10^{-6}$ rds $^{-2}$ Hz $^{-1/2}$	$1.5 \cdot 10^{-8}$ rds $^{-2}$ Hz $^{-1/2}$
Tone (sine at $f_{EP}$ )	$2 \times 10^{-11}$ rds $^{-2}$	Not applicable	Not applicable

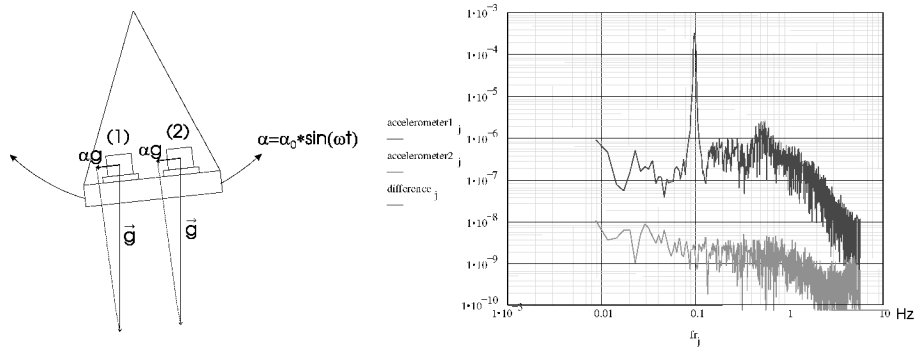


Figure 4. Laboratory calibration of the one axis gradiometer: along the gradiometer axis, the two inertial sensors are submitted to the one  $g$  gravity, projected according to the pendulum bench oscillation ( $\alpha$ ). One of the two sensor outputs is used for the servo-control of the orientation of the pendulum. A sine wave calibrated signal offsets the loop at 0.1 Hz and produces the oscillations. The difference of the two accelerometer outputs (in grey) demonstrates the equality of the sensitivities with a  $10^{-5}$  accuracy and the rejection of the common mode signal (in black).

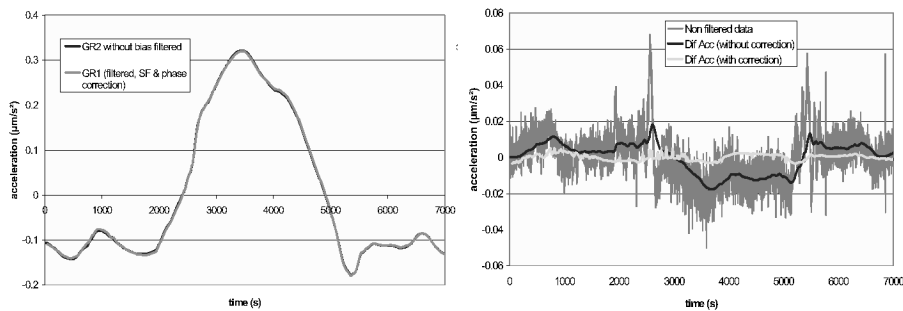


Figure 5. Data provided along track by the two accelerometers on board the GRACE satellites flying on the same orbit at 480 km altitude with 200 km separation. The sensitivities are set with a  $4 \times 10^{-3}$  relative accuracy. The difference of the two outputs are drawn in the right picture, before (in grey) and after (in black and white) filtering. The black and white curves show the adjustment of the sensitivities.

because of larger calibrating signals induced by stronger thrusters (needed however by the low altitude drag) and sustainable by the sensors. The MICROSCOPE satellite is also a 150 kg micro-satellite and procedures and software must be more simple.

The residual drag depends not only on the gain of the drag compensation system loop defining the filtering efficiency but also on the initial level of the atmospheric drag, more than one hundred larger at GOCE orbit altitude. The attitude control is similar in both cases.

## 7. Conclusion

In spite of the fully different scientific objectives of the GOCE mission dedicated to the global and accurate determination of the Earth gravity field and of the MICROSCOPE mission devoted to the test of the Equivalence Principle, these two missions are presently developed on the basis of the same type of electrostatic inertial sensors. Furthermore, the demanded performance of the instruments are very similar and, besides the difference of the geometry of the core, the operation, the involved technology and the limitations are really comparable. Both missions require a satellite with a drag compensation system and a very fine attitude control but the very low altitude of GOCE, as low as 240 km, is much more demanding for the electrical propulsion and the overall sub-system. The accommodation of the sensors needs in both mission a very stiff and steady structure in an insulated thermal case: an active control is envisaged on the GOCE satellite, a fully passive one appears sufficient for MICROSCOPE taking advantage of the weak instrument power dissipation, the Sun synchronous 6–18 hour orbit, the double stage insulation with an external baffled radiator always towards anti-Sun.

The specific difficulty of the GOCE mission is the huge range of measurement, a few  $10^{-6} \text{ ms}^{-2}$  (!), to be met relatively to the very high required resolution of  $10^{-12} \text{ ms}^{-2} \text{ Hz}^{-1/2}$  in the bandwidth from  $5 \times 10^{-3} \text{ Hz}$  to  $10^{-1} \text{ Hz}$ . The MICROSCOPE mission appears therefore easier to be performed with instrument operation at null. Nevertheless, the  $10^{-15}$  EP test accuracy relies in the possibility to integrate during  $10^5$  seconds periods the measured signal in order to reach the detection of acceleration as weak as  $3 \times 10^{-15} \text{ ms}^{-2}$  with the sensor resolution limited to  $10^{-12} \text{ ms}^{-2} \text{ Hz}^{-1/2}$ .

At last, in flight data from the present CHAMP and GRACE satellites show that accelerometers on board satellite are very sensitive to the satellite thermo-elastic behaviour and motion. Figure 5 provides an example of atmospheric drag measurements (along track) by both accelerometers on board the quite identical GRACE satellites flying on the same orbit.

The two curves (left) are very similar and show that the atmospheric density does not vary during the 30 s period between the two satellite passes. The difference of the two curves is drawn with a larger scale (right) showing much more signal oscillations at higher frequency. Clearly, the success of both the MICROSCOPE and the GOCE mission will rely on the soft environment managed on board the satellite and on the filtering ratio that will be obtained in the measurement frequency bandwidth through the differential signal.

## References

- Balmino, G. and Perosanz, F.: 1997, 'Comparison of geopotential recovery capabilities of some future satellite missions', *Proc. IAG symposium, Gravity and Geoid*, p. 403–412.

- Bernard, A., Sacleux, B., and Touboul, P.: 1983, 'GRADIO: orbital gravity gradiometry through differential micro accelerometry', 34<sup>th</sup> IAF Congress, Budapest (Hungary), October 1983, ONERA TP 83 – 18.
- CNES: 2002, 'The French scientific space program', CNES Report to 34<sup>th</sup> COSPAR 2002, CNES publication.
- Damour, T., Piazza, F., and Veneziano, G.: 2002, 'Violations of the equivalence principle in a dilaton-runaway scenario', IHES/P/02/09, Bicocca-FT-02-03, CERN-TH/2002-093, May 2002.
- ESA: 1999, 'Gravity field and steady state Ocean Circulation Explorer mission', ESA SP-1233 (1).
- Fischbach, E. and Talmadge, C. L.: 1998, *The Search for non Newtonian Gravity*, Springer Verlag, 320 pp.
- JPL, GRACE: 1998, 'Gravity Recovery and Climate Experiment — Science and Mission Requirements Document', rev. A, JPLD-15928, NASA's Earth System Science Pathfinder Program 1–84.
- Josselin, V., Touboul, P., and Kielbasa, R.: 1999, 'Capacitive detection scheme for space accelerometers applications Sensors and Actuators A', *Physical*. **78**, 92–98.
- Lämmerzahl, C., Everitt, C. W. F., and Hehl, F. W. (eds.): 2000, *Gyros, Clocks, Interferometers...: Testing Relativistic Gravity in Space, Lecture Notes in Physics*, Springer Verlag, 507 pp.
- McPherson, K. M., *et al.*: 1999, 'A Summary of the Quasi-Steady Acceleration Environment On-Board STS-94 (MSL-1)', AIAA, Reno, USA.
- Nati, M. *et al.*: 1994, 'ASTRE, a highly performant accelerometer for the low frequency range of the microgravity environment', 24<sup>th</sup> Symposium on space environmental control systems, Friedrichshafen, Germany, AIAA Proceedings.
- Reigber, Ch., *et al.*: 1996, CHAMP Phase B Executive Summary, G.F.Z., STR96/13 1–37.
- Reigber, Ch., Lühr, H., Schwintzer, P.: 2002, 'Champ mission status', *Advances in Space Research* **30**(2), 192–134.
- Rummel, R. and Colombo, O. L.: 1985, 'Gravity field determination from satellite gradiometry', *Bull. Geod.* **59**, p. 233–246.
- Tapley, B. and Reigber, C.: 2002, 'The GRACE mission, its status and early results', 34<sup>th</sup> COSPAR, Houston, October 2002.
- Touboul, P.: 2000, 'Space accelerometers: present status', in C. Lämmerzahl, C. W. F. Everitt, F. W. Hehl (eds.), *Gyrod, Clocks, Interferometers...: Testing Relativistic Gravity in Space, Lecture Note in Physics*, Springer Verlag, p. 274.
- Touboul, P. *et al.*: 1991, 'Drag effect on gradiometer measurements', *Manuscripta Geodaetica* **16**(2), 73–91.
- Touboul, P., Foulon, B., and Le Clerc, G.: 1998, 'STAR the accelerometer of the geodesic mission CHAMP', IAF-98-B.3.07.
- Touboul, P., Foulon, B., and Lafargue, L.: 2002, 'The MICROSCOPE mission', *Acta Astronautica* **50**(7), 433–443.
- Willemenot, E. and Touboul, P., 'On-ground investigations of space accelerometers noise with an electrostatic torsion pendulum', *Review of Scientific Instruments* **71**/1, 302–309.